ISSN (Online) 2394-6849

International Journal of Engineering Research in Electronics and Communication Engineering (IJERECE)
Vol 4, Issue 11, November 2017

Energy Based Jiles-Atherton and an Analytical Magnetostrictive Model to Study Response of Terfenol-D Actuator To A Step Input

[1] Shivakumar S Y, [2] Dr. Raghavendra Joshi
[1] Assistant Professor, [2] Professor
Ballari Institute of Technology & Management Bellary, India

Abstract: **- This paper discusses the detailed design aspects and modeling of a magnetostrictive actuator contained coaxial coils surrounding the Terfenol-D rod. Experiments were conducted on this actuator by varying step input under zero pre-stress and pre- stress conditions. The results indicate a better performance of the actuator at each point of excitation when step input is biased to coil 1 instead of varying the step input equally to coaxial coils. The calculation of the magnetic field strength from the actuator coils considers inductance of driving coils. Energy based Jiles-Atherton model is used to predict the magnetization and the quadratic magnetostriction model is improved by considering quality factor in addition to other parameters that affect the output of an actuator. The output, displacement of Terfenol-D rod, obtained with the proposed magnetostriction model was found to have an average deviation of 6 % with respect to experimental results.**

Key words**: Magnetostrictive actuator, Coaxial coils, Step input, Inductance, Jiles-Atherton model, Quadratic magnetostriction model, Quality factor.**

I. INTRODUCTION

Magnetostrictive materials like Terfenol-D have attracted much attention due to excellent magnetostrictive properties. Particularly, the high displacement resolution, high energy density, high frequency bandwidth and short response time makes Terfenol-D material more attractive for sensors and actuators (Anjanappa and Bi, 1994). In line with, the different sensors based on magnetostrictive technology (Calkins, Flatau and Dapino, 2007; Ekreem et al., 2007), few direct and indirect techniques to measure magnetostriction (Ekreem et al., 2007) of a magnetostrictive material used for actuation have been addressed. The prospective use of Terfenol-D has been emerging significantly as it is evident from the various research publications. Based on stimuli generation and configuration in terms of force, stroke and frequency the strategy to select available actuator technologies (Poole and Booker, 2011), analytical approaches to compute magnetic field strength of laminated Terfenol-D eddy current losses into account (Zhifeng, Fuzai and Yang, 2009), electro-mechanical analysis on three types of biased magnetostrictive actuators to explore suitable configuration for providing large biasing fields (Lhermet et al.,1993) have been studied. Apart, the actuator using Terfenol-D material has been employed to neutralize aero elastic and vibration effects in helicopters and fixed wing aircraft (Giurgiutiu, 2000), feasibility of solid-state actuation in helicopter servo-flap for the active control of rotor blade (Giurgiutiu, Rogers and Rusovici, 1996) and emphasized the effect of heat generation from the solenoid that make actuators unreliable used in precision positioning applications (Dozor, 1998). In addition, the modelling of magnetostrictive materials has attracted increasing attention in recent years and considerably developed by improving the existing theoretical models. It is evident from the literature that the strong coupling between magnetic properties and mechanical properties of magnetostrictive materials can be understood through magnetostriction phenomenon. Many researchers have proposed different models to evaluate theoretically the magnetization using Jiles-Atherton field model for ferromagnetic hysteresis (Jiles and Atherton, 1983; 1984; 1986), apart the quadratic moment rotation model for magnetostriction and wave equation for displacement of a Terfenol-D material has been evaluated and showed that these results are in good agreement with the experimental data (Calkins, Smith and Flatau, 2000). This basic approach has been further implemented by Dapino, Smith and Flatau, (2000) and Dapino et al., (2000), in an improved form accounting the effect of applied pre-load on the Terfenol-D (Dapino et al., 2002). To study large deformation produced by magnetostrictive materials, the Euler coordinate system

ISSN (Online) 2394-6849

International Journal of Engineering Research in Electronics and Communication Engineering (IJERECE)
Vol 4, Issue 11, November 2017

and Lagrangian spatial formulation are used for magnetostriction and energy functional (Rogers, 1993), another important characteristic such as blocked force implies the relationship force-displacement capability of a magnetostrictive transducer has been examined (Kellogg and Flatau, 2004). It is evident that the computation of magnetic field before the design phase, experiments to understand clearly the static and dynamic performance and improvisation of available unique models considering few more influencing parameters in order to depict strain accurately are necessary for a Terfenol-D actuator to be designed for specialized application. The present work outlines the design of magnetic circuit of a prototype Terfenol-D actuator. The typical composition of Terfenol-D used in the present work is symbolically represented by . Numerically the magnetic field parameters are evaluated for coaxial coils and actuator assembly with Terfenol-D using Maxwell 2D solver under direct current (DC) driving conditions. Complete comparison of experimental static actuation of an actuator for step input under zero preload and preload are discussed. Magnetization and magnetostriction response are obtained numerically for step input under pre-stress conditions by considering quality factor.

II. COILS FOR THE TERFENOL-D ACTUATOR: SELECTION AND DESIGN

The design of the Terfenol-D actuator requires bias field which could be achieved to the best possible extent using permanent magnets. Engdahl (2002) indicates that the use of permanent magnets in a magnetostrictive actuator for bias field is preferred, when the ratio of length to the radius of Terfenol-D is less than or equal to 3.5. If the ratio exceeds 3.5 the amplitude and homogeneity of bias field decreases drastically. Considering this as the basis, the ratio of length to the radius for the Terfenol-D rod chosen in the present work has 5.7. Moreover, the permanent magnets need to be magnetized and most of their properties will vary significantly with temperature (Brauer, 2006). The use of permanent magnet will depend on the availability of required size and are expensive. This lead to the choice of coil solenoid for the bias magnetic field apart from excitation coil. However, the driving magnetic field produced by a coil used for biasing give rises to eddy current losses. From an application point of view as in the present work, both the coils are energized by the DC input and hence the eddy currents may not be the problem in capturing the desired output of a Terfenol-D actuator.

Design of coils was based on the predetermined strength of the magnetic field to be generated. The strength of magnetic field was calculated using Ampere's law and the same was verified using reluctance approach. One of the typical arrangement of the actuator used in the present work consists of a Terfenol-D rod surrounded by two coaxial coils namely coil 1 and coil 2. The coil 1 will be supplied with a DC input as it is meant for biasing purpose. Superimposed on this is the field produced by coil 2 which will be excited either by DC or alternating current (AC) input. The magnetostriction versus magnetic field curve reported (Engdahl, 2000) for an optimum pre-stress of 6.9 MPa was referred to herein to understand the linear behaviour of Terfenol-D material. For a pre-stress of 6.9 MPa and for an applied field ranging from 48 kA/m to 52 kA/m, the corresponding magnetostriction is 1000-1800 ppm. Considering an average magnetic field strength of 50 kA/m, the number of turns for coil 1 and coil 2 obtained are 560 and 440 to produce a field of 28 kA/m and 22 kA/m. The typical layout of actuator that accommodates Terfenol-D rod and coaxial coils consists of a housing, top end plate and bottom end plate are shown in Figure 1.

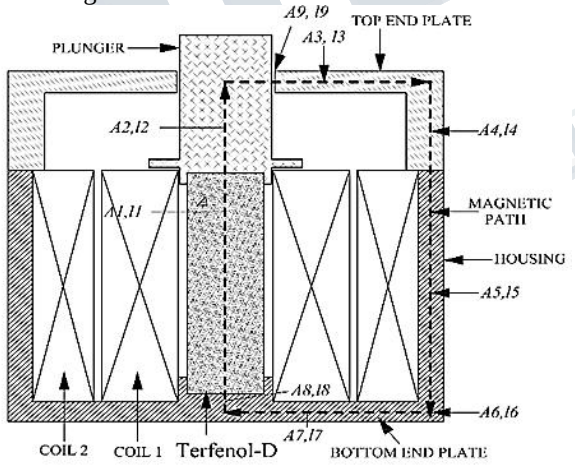

Figure 1. Structure and magnetic circuit of a Terfenol-D actuator.

A. VERIFICATTION OF COIL DESIGN WITH RELUCTANCE APPROACH

In a DC field, the reluctance is the ratio of the magneto-motive force (MMF) in a magnetic circuit to the magnetic flux in this circuit. The number of turns calculated for coaxial coils of a Terfenol-D actuator under DC input is verified by reluctance approach. Mathematically the reluctance is given by:

$$\Re = \frac{\text{MMF}}{\phi} \qquad (1)$$

Where $\Re$ is the magnetic reluctance in AT/Wb, MMF is magneto motive force in Ampere-turns and ϕ is magnetic flux in Webers.

Magnetic flux always forms a closed loop as described by Maxwell's equations, but the path of the loop depends

ISSN (Online) 2394-6849

International Journal of Engineering Research in Electronics and Communication Engineering (IJERECE)
Vol 4, Issue 11, November 2017

on the reluctance of the surrounding materials. It is concentrated around the path of least reluctance. Air and vacuum have high reluctance, while easily magnetized materials such as soft iron have low reluctance. The concentration of flux in low-reluctance materials forms strong temporary poles and causes mechanical forces that tend to move the materials towards regions of higher flux so it is always an attractive force.

The reluctance of a uniform magnetic circuit can be calculated as:

$$\Re = \frac{l}{\mu_0 \ \mu_r \mathrm{A}} \qquad (2)$$

Where l is a length of each component in meters, μ_0 is the permeability of vacuum in H/m, μ_r is the relative magnetic permeability of the material and A is the cross-sectional area of each component in a magnetic circuit.

According to Ampere's law the relationship between the current (I) and magnetic field intensity (H) can be expressed as:

$$H = \frac{NI}{l} \qquad (3)$$

Substituting for l from Equation (2) in to Equation (3), the number of turns for coil is given by (Grunwald and Olabi, 2008):

$$N = \frac{\Re \mu_0 \mu_{r(Terfenol-D)} H_{Terfenol-D} \mathrm{A}_{Terfenol-D}}{I} \qquad (4)$$

Where $H_{Terfenol-D}$ is a magnetic field exerted on Terfenol-D rod, $\mathrm{A}_{Terfenol-D}$ is the cross-sectional area of Terfenol-D rod and I is an applied DC input in amperes.

Assuming that the driving coils of the actuator are required to operate on a maximum DC input of 4 A, the corresponding size of copper wire chosen was 17 SWG (BS6722, 1986). Using Equation (4) along with reluctances of individual components listed in Table 1, the number of turns for coil 1 and coil 2 has been calculated. The number of turns for coil 1 will be 567 turns and 454 turns for coil 2 to produce 28 kA/m of biasing magnetic field and 22 kA/m of peak magnetic field respectively which are in close agreement to 560 and 440 that obtained using Ampere's law.

B. Magnetic Circuit Optimization of a Terfenol-D Actuator

The magneto motive force generated by the coaxial coils should act over the entire length of the Terfenol-D rod in order to improve the efficiency of energy conversion. Besides, the magnetic flux lines produced by the coils should take their path along the Terfenol-D rod. The magnetic resistance of the magnetic circuit should be minimized, especially the resistance of the actuator housing to improve the magnetic flux. Engdahl (2000) and Brauer (2006) emphasize certain aspects related to the optimization of magnetic circuit of a Terfenol-D actuator and they are as follows:

i) Magnetic field being generated should take a path so that flux lines can reach the measuring end of rod where output is desired.

ii) Components of actuator assembly such as housing, top and bottom end plate should be manufactured with the soft magnetic materials which have high magnetic conductivity.

iii) Surface area of the housing, top and bottom end plate should be increased as much as possible for a given volume of the actuator.

iv) The magnetic circuit should be closed.

v) Thickness of air gap between housing and coaxial coils, and between coil and Terfenol-D rod in an actuator arrangement should be reduced as much as possible.

The magnetic conductivity of Terfenol-D material is in between 4-12 (Engdahl, 2000). It is smaller than other individual components of an actuator. The magneto motive force produced by the coaxial coils should act effectively on Terfenol-D rod. Hence the driving coils are to be designed as hollow in cross-section. The electric-magnetic turnover ratio is to be improved as much as possible and energy consumed by coils must be very small so that heat generated by the coaxial coils will be minimized in order to meet the requirement of magnetic field strength produced by the coils. This electric-magnetic turnover ratio depends on coil geometry. Therefore the geometry of the coaxial coils is to be optimized and it is carried out considering four parameters namely inside and outside radii of coils, length and shape of the coils.

According to the application of actuator, geometric parameters of the Terfenol-D rod can be determined and corresponding radii of the coils and lengths are also to be determined.

Considering the coil losses, the magnetic field inside the hollow coil (Engdahl, 2000) is given by

$$H_{coil} = G_{coil} NI \sqrt{\frac{\pi}{l_{coil} a_1} \times \frac{(\alpha+1)}{(\alpha-1)}} \qquad (5)$$

Where G_{coil} is the shape factor of magnetizing coil.

$$G_{coil} = G_{coil}(\alpha,\beta) = \frac{1}{5}\left[\frac{2\pi\beta}{\alpha^2-1}\right]^{1/2} \log_e \left[\frac{\alpha+(\alpha^2+\beta^2)^{1/2}}{1+(1+\beta^2)^{1/2}}\right] \qquad (6)$$

ISSN (Online) 2394-6849

International Journal of Engineering Research in Electronics and Communication Engineering (IJERECE)
Vol 4, Issue 11, November 2017

$\alpha = \frac{a_2}{a_1}$

a_1 and a_2 are inner and outer radii of the coils in

$\beta = \frac{l_{coil}}{2a_1}$

and .

The magnetic field at the center of each coil can be represented using Equation (5) as follows by:

$$H_{coil1} = 1.06\frac{NI}{l_{coil}} \quad \text{and} \quad H_{coil2} = 0.829\frac{NI}{l_{coil}} \qquad (7)$$

Equation (7) represents the most efficient design with respect to the dissipated power in the coaxial coils. From the Equation (5), it is observed that the magnetic field is large at the center of the coil. The magnetic field declines rapidly towards the ends of the coil (Wang et al., 2006). Therefore the length of the coils should be slightly larger than the length of the Terfenol-D rod. The length of coaxial coils was assumed as 83 mm. With a view to reduce the magnetic leakage, the inner radius of the coil 1 was chosen close to the radius of the Terfenol-D rod. The inner radius of the coil 2 should be approximately equal to the outer radius of coil 1. The radius of the Terfenol-D rod was chosen to be 14 mm.

With this the length and inside radii of the coils are fixed, the objective will be to determine the optimum values of outer radii of coils. The analytical treatment discussed in Dehui, Quanguo and Yuyun (2008) is followed to optimize the outside radii of coils. Leakage of magnetic flux in a magnetic circuit can be accounted in the Ampere's theorem by means of compensation coefficient of the drive coil K_{coil} (Engdahl, 2000; Dehui, Quanguo and Yuyun, 2008) as follows,

$$NI = K_{coil} H_{coil} L_T \qquad (8)$$

Further, comparing the Equation (7) and (8), the coil compensation coefficient for each coil listed in Table 2 is computed and used in the optimizing criteria that verifies the outer radii of coaxial coils.

According to the definition for current density of the coil:

$$J = \frac{NI}{\mathrm{A}_{coil}} = \frac{K_{coil} H_{coil} L_T}{\mathrm{A}_{coil}} \qquad (9)$$

Where A_{coil} = area of coil and L_T = length of Terfenol-D rod. In practical application the current density of coil under the different work system are as follows: for long duration of operation J has a range of 2×10-6 to 4×10-6A/m2; when actuator has to undergo intermittent operation J has a range of 5×10-6 to 12×10-6 A/m2; and finally for short duration of operation the current density J is 13×10-6 to 30×10-6 A/m2. In the present work the current density for long term operation was assumed, then requirement on the area of the coil A_{coil} is

$$\frac{K_{coil} H_{coil} L_T}{4\times10^{-6}} \le \mathrm{A}_{coil} \le \frac{K_{coil} H_{coil} L_T}{2\times10^{-6}} \qquad (10)$$

The outside radii of both coils are to be optimized by meeting constraints of Equation (10). Therefore the coil design will be based on an optimized value of the shape of the coil and cross-sectional area of the coil as follows,

$$\left\{ \mathrm{Max}\, G_{coil}(\alpha,\beta);\ \frac{K_{coil} H_{coil} L_T}{4\times10^{-6}} \le \mathrm{A}_{coil} \le \frac{K_{coil} H_{coil} L_T}{2\times10^{-6}} \right\} \qquad (11)$$

Optimization for coil 1 is as follows:

$$\{\mathrm{Max}(0.16349);\ 5.8\times10^{-4} \le 7.47\times10^{-4} \le 1.162\times10^{-3}\}$$

Hence the optimum outside diameter of coil 1 is 36.5 mm which satisfies the optimization criterion.

Optimization for coil 2 is as follows:

$$\{\mathrm{Max}\ (0.14425);\ 4.56\times10^{-4} \le 5.81\times10^{-4} \le 9.13\times10^{-4}\}$$

Hence the optimum outside diameter of coil 2 is 57.5 mm which satisfies the optimization criterion

The maximum fabry factor G_{coil} for coil 1 is 0.16349 with $\alpha = 2.2121$, $\beta = 2.5151$ and for coil 2 is 0.14425 with $\alpha = 1.5333$, $\beta = 1.1067$ indicates the geometry of coaxial coils, in which the magnetic field produced by them are for the least dissipated resistive power (Engdahl, 2000). Table 2 lists the hollow coil dimensions obtained as per the magnetic field intensity requirement

III. RESPONSE OF A TERFENOL-D: A EXPERIMENTAL SET UP

The schematic and experimental set-up shown in Figure 2 (a) and (b) illustrates the Terfenol-D rod surrounded by coaxial coils together placed in a mild steel housing. Opto NCDT 1402 laser displacement sensor was held by means of a digital vernier height guage and used to measure the displacement of a Terfenol-D actuator. The laser displacement sensor Opto NCDT 1402 provides a resolution of 1 µm for static measurements and has a frequency response of 1.5 kHz. The output from the displacement sensor is communicated to the computer using RS422 USB serial converter and is processed by the ILD 1402 v2.03 software. The coaxial coils are energized by a regulated dual power supply unit. The S9 HBM force transducer with load range of 0-10 kN was used to monitor the load being applied on Terfenol-D rod during experimentation on actuator under prestress conditions

ISSN (Online) 2394-6849

International Journal of Engineering Research in Electronics and Communication Engineering (IJERECE)
Vol 4, Issue 11, November 2017

(corresponding prestress range of 0-6.9 MPa). It was interfaced to IBM Z60t laptop through Lab

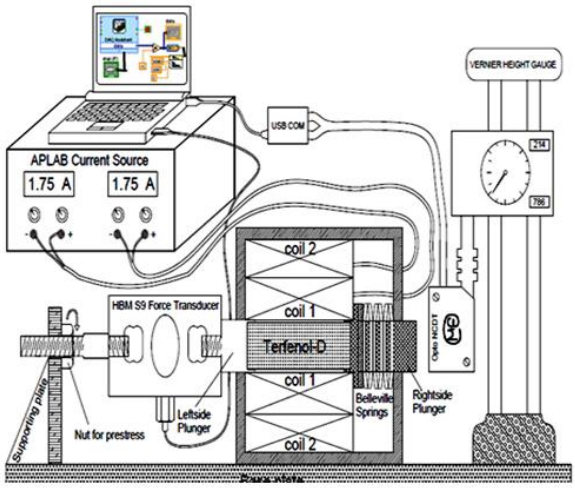

Figure 2(a) . Schematic setup of a Terfenol-D actuator.

Figure 2 (b). Experimental set up of a Terfenol-D actuator

VIEW software using NI 9237 module. This module gives output in terms of load with respect to the load applied on the Terfenol-D rod. Force transducer data was collected at a continuous sampling rate of 25000 samples per second with a frequency of 25000 Hz using low pass filter. Low pass filter known as inverse Chebyshev filter was used to capture the output from the transducer without signal noises at a desired frequency. An inverse Chebyshev low pass filter was used with the following specifications: Order 2, lower cutoff frequency 1 Hz, higher cutoff frequency 100 Hz and sampling frequency of 1000 Hz.

IV. MAGNETOSTRICTIVE ACTUATOR UNDER THE ACTION OF MAGNETIC FIELD AND APPLIED PRE-STRESS

Analytical expressions for evaluating magnetic field strength taking inductance of driving coils in to account, magnetization and displacement of Terfenol-D rod are presented keeping in mind a step input to the coil(s).

A. Magnetic field strength in a Terfenol- D actuator

The magnetic flux density (B) is related to the magnetic field intensity (H) as:

$$B = \mu^{\sigma} H \tag{12}$$

Where B is a magnetic flux density distribution on Terfenol-D rod in Tesla, μ^{σ} is the relative magnetic permeability at a constant stress and H is a magnetic field intensity distribution on Terfenol-D rod for an applied input to a coil in kA/m. Further the inductance of driving coils is considered to frame the distribution of magnetic field intensity on Terfenol-D rod. The concept of inductance originates from Faraday's law and represents the relationship between the counter emf induced to the current supplied to the coil. Different factors like number of turns, core material, length and area of coils will dictate the inductance that affects the magnetic flux distribution over the length of Terfenol-D rod. The inductance (L) of coil is a function of input current and applied pre-stress (Liyi et al., 2011; Gupta, 2004). Thus the magnetic flux density distribution on Terfenol-D rod in terms of inductance can be expressed as:

$$B = L \,.\, I / N A_{Terfenol-D} \tag{13}$$

Substituting the magnetic flux density of Equation (13) into Equation (12) gives:

$$H = \frac{L \,.\, I}{N A_{Terfenol-D} \mu^{\sigma}} \tag{14}$$

When the actuator coil is excited with step input, the current (I) rises exponentially (Brauer, 2006) and is given by

$$I = I_{dc}\left[1 - e^{\frac{-t}{\tau}}\right] \tag{15}$$

On substituting Equation (15) into Equation (14), the magnetic field strength from the actuator coil for step input is given by

$$H = \frac{L \,.\, I_{dc}\left[1 - e^{-\frac{t}{\tau}}\right]}{N\ A_{Terfenol-D}\ \mu^{\sigma}} \tag{16}$$

ISSN (Online) 2394-6849

International Journal of Engineering Research in Electronics and Communication Engineering (IJERECE)
Vol 4, Issue 11, November 2017

Where I_{dc} is steady state current to a coil, t is time and $\tau = \frac{L}{R}$ has the units of time, L and R are the inductance and resistance of the coil.

However, when there are two coils either connected in series or separated by short distance with different magnitudes of current input, then the total inductance of each coil will differ. Inductance in such a case is due to the contribution of self-inductance and mutual inductance. The induced emf in a coil due to current flowing in a same coil is self-inductance L_s and emf inducing in a coil due to current flowing in nearby coil is known as mutual inductance L_m. Therefore the total inductance L of a coil is,

$$L = L_s + L_m$$

The self-inductance (L_s) of a coil (Olabi and Grunwald, 2008) is given by:

$$L_s = \mu_0 \frac{\pi^2}{6} G_{coil}^2 N^2 a_1 (\alpha+1)(\alpha+3) \quad (17)$$

Where μ_0 is permeability of a material in free space, G_{coil} depends on shape and cross-section of coil given in Equation (6), N is number of turns of coil 1 or coil 2.

Similarly the mutual inductance (L_m) can be expressed as (Young, Freedman and Ford, 2007):

$$L_m = \frac{\mu_0 N_1 N_2 A_{coil}}{l_{coil}} \quad (18)$$

Where N_1 and N_2 are number of turns in coil 1 and coil 2, A_{coil} and l_{coil} are the cross-sectional area and length of coil. In the present work, the Terfenol-D actuator consists of two coils coaxially placed with a small clearance between them. Based on the selected layout for the actuator, the inductance of each coil is the resultant of Equation (17) and Equation (18). Therefore the total inductance of coil 1 (L_1) is equal to the sum of self-inductance of coil 1 and mutual inductance of coil 2 with respect to coil 1 as,

$$L_1 = L_{s1} + L_m = \mu_0 \frac{\pi^2}{6} G_{coil1}^2 N_1^2 a_1 (\alpha+1)(\alpha+3) + \frac{\mu_o N_1 N_2 A_{coil1}}{l_{coil}} \quad (19)$$

Similarly the total inductance of coil 2 (L_2) is equal to the sum of self-inductance of coil 2 and mutual inductance of coil 1 with respect to coil 2 as,

$$L_2 = L_{s2} + L_m = \mu_0 \frac{\pi^2}{6} G_{coil2}^2 N_2^2 a_1 (\alpha+1)(\alpha+3) + \frac{\mu_o N_1 N_2 A_{coil2}}{l_{coil}} \quad (20)$$

The maximum magnetic field strength is equal to the sum of field strength distribution on Terfenol-D by coil 1 and coil 2 and thus evaluated by the following expression,

$$H = \frac{L_1(\sigma, I) I_1 \left[1 - e^{-\frac{tR_1}{L_1}}\right]}{N_1 A_{Terfenol-D} \mu^{\sigma}} + \frac{L_2(\sigma, I) I_2 \left[1 - e^{-\frac{tR_2}{L_2}}\right]}{N_2 A_{Terfenol-D} \mu^{\sigma}} \quad (21)$$

B. Evaluation of magnetization using Jiles-Atherton model

Magneto-mechanical hysteresis curves of a Terfenol-D actuator for DC input under pre-stress conditions are analyzed using Jiles-Atherton theory (Jiles and Atherton, 1984). It is a hysteretic model describing the relationship between external magnetic field intensity and magnetization. Magnetic flux density and magnetization of a Terfenol-D change under the action of a force. Based on assumption that hysteresis originates primarily from domain wall pinning and the release of domain walls from their pinning sites cause the magnetization to change in such way as to approach the anhysteretic state. The anhysteretic magnetization is figured through consideration of the thermodynamic properties of the magnetostrictive material.

The J-A model of hysteresis starts with anhysteretic magnetization in which coupling of field and inter domain magnetization are formulated using mean field theory. The magnetization in response to this effective field for a ferromagnetic material can be expressed as:

$$M = M_s f(H_e) \quad (22)$$

Where H_e is an effective magnetic field given by Equation (21), M_s is a saturation magnetization of a Terfenol-D material and f is an arbitrary function of effective field. Impurity sites and non-magnetic inclusions are not considered in the model. This is true in case of ideal material in which impedance to the domain wall motion is in the form of pinning sites. In actual practice the presence of pinning sites are unavoidable. Equation (22) describes only the anhysteretic curve or ideal magnetization curve in practice and can be expressed as:

$$M_{an}(H_e) = M_s f(H_e) \quad (23)$$

Where M_{an} is an anhysteretic magnetization. Jiles and Atherton used the Langevin function to suit the shape of anhysteretic curve to calculate anhysteretic magnetization as follows:

ISSN (Online) 2394-6849

International Journal of Engineering Research in Electronics and Communication Engineering (IJERECE)
Vol 4, Issue 11, November 2017

$$M_{an}(H_e) = M_s\left(\coth\left(\frac{H_e}{a}\right) - \left(\frac{a}{H_e}\right)\right) \quad (24)$$

Where a is a shape parameter of anhysteretic curve. Pinning sites have the effect to decrease the initial permeability $\left(\frac{\partial M}{\partial H}\right)$ of a ferromagnetic material and increase its coercive force. By considering pinning sites into account the resulting magnetization referred as irreversible magnetization M_{irr} can be written as:

$$M_{irr} = M_{an} - \delta k\left(\frac{dM_{irr}}{dB_e}\right) \quad (25)$$

Where k is a pinning constant, δ is a parameter which takes on value +1 when H increases in the positive direction which means that $\frac{dH}{dt} > 0$ and it takes values −1 when H increases in negative direction i.e. $\frac{dH}{dt} < 0$. Solving and rearranging Equation (25) the irreversible magnetization change in the material can be expressed as (Jiles and Atherton, 1984):

$$M_{irr} = M_s\left\{\mathcal{L}\left(\frac{H_e}{a}\right) - (k\delta)\left(\mathcal{L}^{1}\left(\frac{H_e}{a}\right) - \mathcal{L}^{1}\left(\frac{H_{\max}}{a}\right)\right) + (k\delta)^2\,\mathcal{L}^{2}\left(\frac{H_e}{a}\right)\right\} \quad (26)$$

Depending on the order of the derivative that encompasses the series, the solution of M_{irr} will vary. Reversible magnetization of the material can be written in terms of irreversible magnetization and anhysteretic magnetization as:

$$M_{rev} = c\left(M_{an} - M_{irr}\right) \quad (27)$$

Where c is called reversible coefficient.

Further total magnetization is evaluated as the sum of reversible and irreversible magnetization. The total magnetization equals to

$$M_{tot} \text{ or } M = M_{rev} + M_{irr} \quad (28)$$

C. Description, improvisation and evaluation of magnetostriction with quality factor

The magnetostriction $\lambda = dL_T / L_T$ specifies the relative change in the length of the material from the ordered, but unaligned state to the state in which domains are aligned. The magnetostriction does not quantify the effects of domain order or thermal effects. It provides a measure of the strains generated in a Terfenol-D material. Assuming the pre-stress is sufficiently large, magnetostriction can be approximately represented as a single valued function of magnetization (Calkins, Smith and Flatau, 2000) as:

$$\lambda = \frac{3}{2}\frac{\lambda_s}{M_s^2}M^2 \quad (29)$$

Equation (29) represents as a first approximation to the relationship between the magnetization and magnetostriction in isotropic materials. In Equation (29), λ_s is saturation magnetostriction and M_s is saturation magnetization.

An extensive workout has been done by many researchers to improve the quantification of magnetostriction. Defining Gibbs-free energy as function of stress, magnetic field and temperature and applying Taylor's series on Gibbs-free energy Carman and Mitrovic (1995) have derived non-linear constitutive relations for dependent variables like strain, temperature and magnetic field. Yongping et al. (2003) and Wan, Fang and Hwang (2003) have developed hierarchical magnetostriction non-linear constitutive models using the Gibbs free energy and the one based on providing a mathematical description for domain activity. The simplest among them was the standard square model, obtained by series expansion of the Gibbs free energy. This non-linear constitutive model predicted magnetostriction very well for low and moderate magnetic fields. This was improved by adopting hyperbolic tangent function in the Gibbs free energy and was referred to as hyperbolic tangent constitutive relations. This model tries to predict magnetostriction reasonably well for high magnetic fields. Finally Wan, Fang and Hwang (2003) adopted the magnetic domain behaviour mathematically by defining domain density switching function. The domain motion is due to magnetic field as well as applied prestress. Thus incorporating the domain switching density function in the Gibbs free energy, constitutive relations are derived that embodies the switching activity of the magnetic domains. The most notable work on the development of non-linear constitutive model for Terfenol-D rod in the recent times is from Zheng and Liu (2005). The constitutive model of Zheng and Liu can be applied to magnetostrictive material that exhibit the positive and negative magnetostriction. Further various parameters like relaxation factor, initial and saturation Young's modulus, saturation magnetostriction and saturation magnetization which are the inputs for the model can be easily obtained from experiments. Apart the model takes in to account the variation of Young's modulus due to magnetic field and the applied load. Zheng and Liu have proved that the constitutive model developed provide good results for low, moderate and high magnetic fields. Zheng and Liu's model has been adopted by many researchers, Zhou, Zhou

ISSN (Online) 2394-6849

International Journal of Engineering Research in Electronics and Communication Engineering (IJERECE)
Vol 4, Issue 11, November 2017

and Zheng (2007) and Yong and Lin (2009), to study the performance of Terfenol-D rod for actuator application. The analytical constitutive model for magnetostriction accounting the prestress as well as ΔE effect from Zheng and Liu is as follows:

$$\lambda = \frac{\sigma}{E_s} + \frac{\lambda_s}{2}\tanh\left(\frac{2\sigma}{\sigma_s}\right) + \left(1 - \frac{1}{2}\tanh\frac{2\sigma}{\sigma_s}\right)\lambda_s\left(\frac{M}{M_s}\right)^2 \quad (30)$$

In addition to the above said parameters, the quality factor is one of the key parameter influencing the output strain of a Terfenol-D actuator (Engdahl, 2000; Olabi and Grunwald, 2008) and thus will be taken into account in the magnetostriction model. It is generally recommended to use Terfenol-D under pre-load to obtain high magnetostriction with same magnetic field. Strain is strongly dependent on the application of both magnetic field and pre-stress (Claeyssen et al., 1997), while Young's modulus of the material also changes with local stress in the rod (Zhou, Zhou and Zheng, 2007). Second, the Terfenol-D material can support little tensile or shear load. Thus to avoid a risk of tensile loading, a prestress is usually required (Karunanidhi and Singaperumal, 2010). Consider the operation of Terfenol-D rod to an applied step input. During the transient, the blocked force and the applied preload can vary. Apart the rod is likely to undergo longitudinal oscillation. However, the Terfenol-D rod possesses a resonance frequency in the longitudinal direction. To observe this, the Terfenol-D rod must be free to vibrate by operating an actuator under no load conditions. These factors call upon to adopt the dynamic strain coefficient in the magnetostriction model. The strain at resonance is much higher than it is under quasi-static conditions (Claeyssen et al., 1997; Olabi and Grunwald, 2008). The strain at resonance condition is given by:

$$\lambda_{33} = Q_3 d_{33} H \quad (31)$$

Where Q_3 is an amplification factor known as quality factor, the coefficient d_{33} is called dynamic strain coefficient and it is independent of the longitudinal frequency. Assuming zero prestress and as well as linear relationship between λ and H, then quality factor Q_3 will be unity and H is an applied magnetic field on Terfenol-D from coaxial coils.

In actual practice though the devices using Terfenol-D being designed in a linear region, the behaviour of Terfenol-D material will be non-linear due to inherent property of magnetostrictive material. This brings the existence of non-linear relationship between strain and magnetic field. Under these circumstances, the quality factor (Q_3) will exists in Equation (31) whose value ranges from 3 to 20 (Olabi and Grunwald, 2008) and magnetic field is due to applied prestress denoted by H_σ whose expression reported in Sun and Zheng (2005) and Yong and Lin (2009) apart from coaxial coils.

In the present work, the magnetostriction is computed by combining Equation (30) and Equation (31) for a Terfenol-D actuator as follows.

$$\lambda = \frac{\sigma}{E_s} + \frac{\lambda_s}{2}\tanh\left(\frac{2\sigma}{\sigma_s}\right) + \left(1 - \frac{1}{2}\tanh\frac{2\sigma}{\sigma_s}\right)\lambda_s\left(\frac{M}{M_s}\right)^2 + Q_3 d_{33} H \quad (32)$$

Where H is the resultant magnetic field due to the coil and due to applied prestress. The field due to applied prestress is as follows (Sun and Zheng, 2005; Yong and Lin, 2009),

$$H_\sigma = \left\{4\sigma - \sigma_s \ln\left[\cosh\left(\frac{2\sigma}{\sigma_s}\right)\right]\right\}\frac{\lambda_s M}{2\mu_0 M_s^2}$$

Substituting H_σ in Equation (33) and rearranging yields,

$$\lambda = \frac{\sigma}{E_s} + \frac{\lambda_s}{2}\tanh\left(\frac{2\sigma}{\sigma_s}\right) + \left(1 - \frac{1}{2}\tanh\frac{2\sigma}{\sigma_s}\right)\lambda_s\left(\frac{M}{M_s}\right)^2 + \left\{4\sigma - \sigma_s \ln\left[\cosh\left(\frac{2\sigma}{\sigma_s}\right)\right]\right\}\frac{\lambda_s M}{2\mu_0 M_s^2} \quad (33)$$

D. Numerical study of magnetic flux density in coaxial coils and Terfenol-D actuator

Coaxial coils in free air and actuator assembly with and without Terfenol-D are energized with DC input to analyze the magnetic flux density using the finite element analysis. The fundamental equation for finite element analysis of linear magnetostatic (DC magnetic) fields is expressed as (Brauer, 2006):

$$\frac{\partial}{\partial \mathbf{A}}\left(\int \frac{B^2}{2\mu} dv - \frac{1}{2}\int \mathbf{J} dv\right) = 0 \quad (34)$$

Where B is a magnetic flux density, μ is the permeability of a material, $\mathbf{A}$ is the magnetic vector potential and J is the current density.

The numerical solution to the magnetostatic equation given by Equation (34) is obtained by Maxwell 2D solver v5. The axi-symmetric models for the coaxial coils in free air and Terfenol-D actuator assembly needs to be created in Maxwell 2D solver. The domain of solution is defined as the assembly of the actuator with background domain as air. The model of Terfenol-D actuator assembly with coaxial coils was discretized with triangular finite elements using Maxwell 2D solver is shown in Figure 3. Maxwell 2D solver presents a

ISSN (Online) 2394-6849

International Journal of Engineering Research in Electronics and Communication Engineering (IJERECE)
Vol 4, Issue 11, November 2017

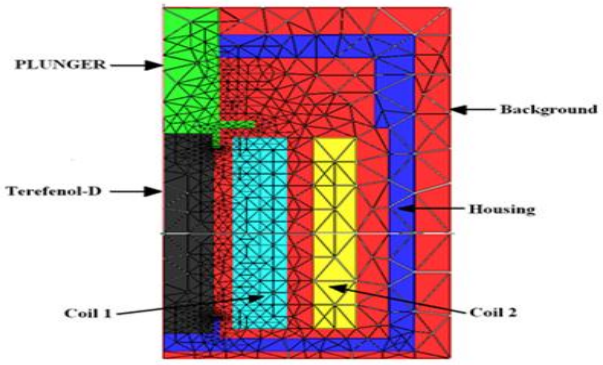

Figure 3. Discretization of the actuator assembly with coaxial coils using triangular finite elements in a Maxwell 2D solver.

solution setup of the adaptive mesh analysis type. Thus the mesh refinement was carried out within the solver such that number of passes was chosen as 10 with 1 % refinement. With this, number of triangular elements used were 1647, energy error was 0.8 % for a converged solution.

V. RESULTS AND DISCUSSION

Magnetic flux density of coaxial coils and actuator assembly with Terfenol-D rod is presented and analyzed. Experimental response of Terfenol-D rod for a step input is described. Magnetostriction of Terfenol-D is analyzed by varying the input to coil 1 and coil 2 independently and simultaneously. Using Jiles- Atherton model, quadratic magnetostriction model and alternate proposed model for magnetostriction is used to present magnetization and magnetostriction response for step input. Finally the theoretical and experimental time response of Terfenol-D actuator will be compared. Energy output from the Terfenol-D actuator is also evaluated.

A. Comparison of flux density of coaxial coils in free air

Figure 4 shows the comparison of axial flux density measured in the absence and presence of Terfenol-D within the coaxial coils in free air. It is observed that the magnetic flux density increases as the applied input increases to the coils in free air.The magnetic flux density is increasing linearly in the absence of Terfenol-D rod, shows non-linear behaviour in the presence of Terfenol-D rod. This may be due to the presence of air gap between coils and Terfenol-D, results in disturbance for the continuous and uniform flow of magnetic flux from the coils and Terfenol-D. Magnitude of the flux density is large when the Terfenol-D rod is placed within the coil. It is also observed that the magnetic flux distribution is stronger by 67 % when the actuator is contained with Terfenol D.

B. Distribution of axial and radial magnetic flux density in the actuator

Figure 5 shows the axial and radial magnetic flux density distribution in an actuator with mild steel housing in the presence of Terfenol-D. The current density input to the coil 1 and coil 2 are 1350 and 1060 kA/m2 for 4 A respectively. It is observed that the axial magnetic flux density increases from either ends and remains uniform inside the coil with Terfenol-D.

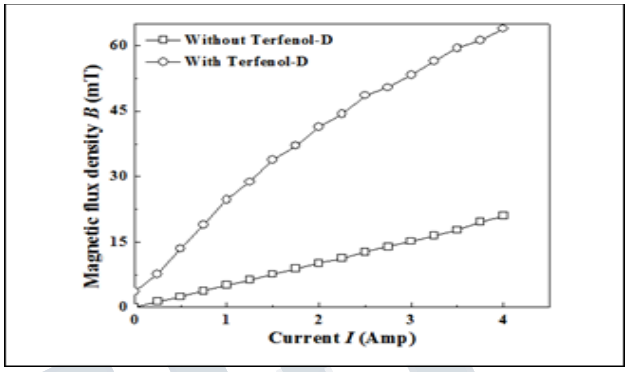

Figure 4. Comparison of magnetic flux density in a coaxial coils with and without Terfenol-D.

The radial magnetic flux distribution has discontinuities due to the presence of various materials. The radial magnetic flux density is uniform in air. When the Terfenol-D rod is present in the actuator, the radial flux density immediately falls sharply and decreases linearly due to presence of coils, bobbin material and wall of the housing as shown in Figure 5.

C. Flux distribution in a Terfenol-D actuator

The distribution of flux in an actuator assembly with Terfenol-D rod has been discussed. The intensity and magnitude of a flux lines in an actuator assembly with Terfenol-D are dense and high have been observed. When the Terfenol-D is present in the actuator assembly, the flux lines are drawn heavily towards the Terfenol-D and coil 1 as evident from Figure 6.

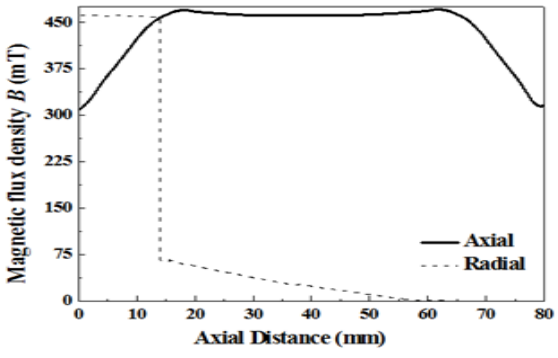

Figure 5. Axial and radial magnetic flux density distribution in an actuator assembly with Terfenol-D.

ISSN (Online) 2394-6849

International Journal of Engineering Research in Electronics and Communication Engineering (IJERECE)
Vol 4, Issue 11, November 2017

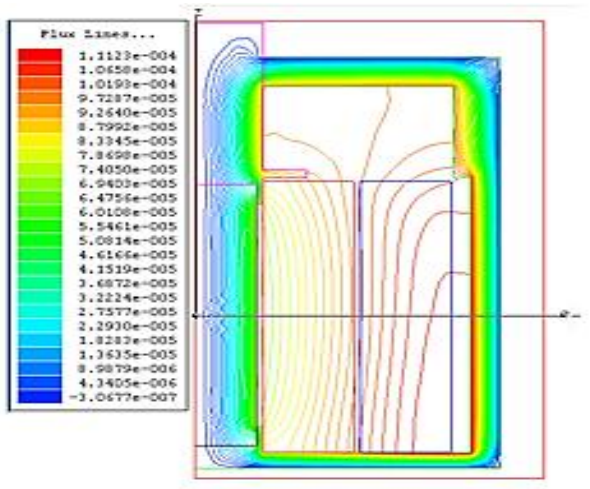

Figure 6. Comparison of flux distribution in an actuator assembly with mild steel housing with Terfenol-D.

This is due to high relative permeability of housing made of mild steel material $(\mu_r = 4000)$ compared to permeability of active material $(\mu_r \approx 4-12)$ in the presence of Terfenol-D. The relative permeability of a Terfenol-D rod used in the present work is equal to 7.

D. Experimental response curves of a Terfenol-D actuator

Experiments are conducted with Terfenol-D actuator for a DC input of 0 A to 4 A in a step of 0.25 A under pre-stress conditions. Typical response curves obtained by varying DC input to both coils using laser displacement sensor are shown in Figure 7 (a, b, c and d).

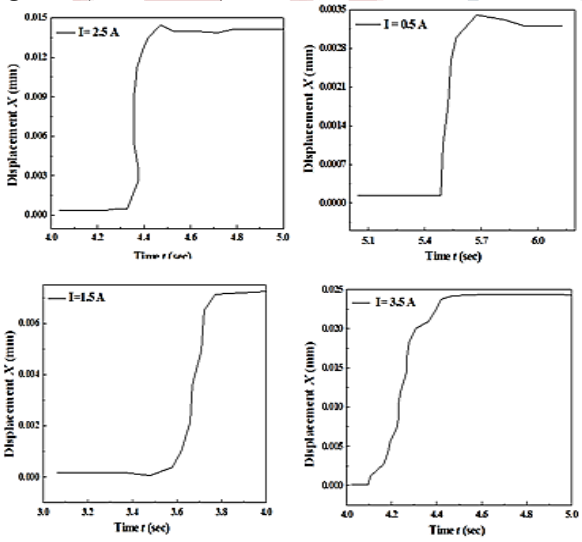

Figure 7. Response of Terfenol-D actuator under zero pre-stress for step input of (a) 0.5 A (b) 1.5 A (c) 2.5 A and (d) 3.5 A to coaxial coils.

A step response is observed from the point of excitation to reach maximum for a given input and thereafter the magnitude is constant. It is observed that the output attains a maximum and remains steady. The output has a form similar to that of a step. The steady state displacement was found to be 0.0031, 0.0093, 0.0156 and 0.0255 mm (3.1, 9.3, 15.6 and 25.5 µm) for a DC input of 0.5 A 1.5 A, 2.5 A and 3.5 A respectively.From the experimental response displacement it is observed that there is finite time to reach the maximum input from zero. The time to reach the maximum output is 333, 568, 273 and 326 ms for step input of 0.5, 1.5, 2.5 and 3.5 A respectively. It is also observed that the response time of actuator from the point of excitation to steady state point is increasing as the input increases.

Figure 8 (a) shows hysteresis in the output of Terfenol-D actuator. The experiment was conducted for one completer cycle (i.e. increasing and decreasing) and the data was collected at a frequency of 1 kHz. The step input is increased from 0 to 4 A and again decreased to 0 A in steps of 0.25 A equally to coaxial coils of a Terfenol-D actuator. Each time the step input was applied and brought back to zero. Three trials were taken for each input operating condition and the average obtained during increasing and decreasing case have been plotted. The difference between the measured points for increasing and decreasing cases are close to 1 µm, which is the resolution of the laser displacement sensor. Mean sum of square of error is 2 between the experimental displacement during the increase and decrease of step input to coaxial coils. This may be also due to the measurement noise for the deviation obtained. In addition, this may be due to inherent property of Terfenol-D material as it depends on electron spin, orientation and interaction of spin orbitals and the molecular lattice configuration. Figure 8 (b) shows the strain induced in a Terfenol-D actuator by varying the step input to coaxial coils. Its behaviour is similar to the one discussed with respect to the Figure 14. The maximum strain of 373 ppm at an applied step input of 4 A has been achieved.

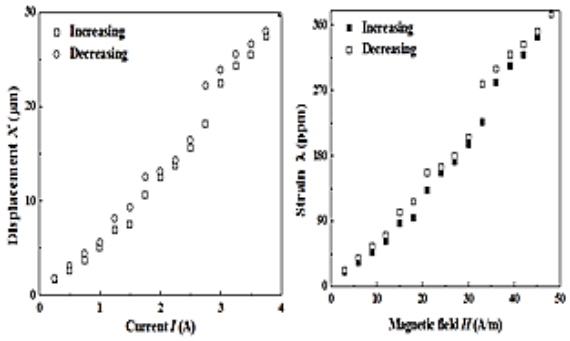

ISSN (Online) 2394-6849

International Journal of Engineering Research in Electronics and Communication Engineering (IJERECE)
Vol 4, Issue 11, November 2017

Figure 8. (a) Displacement and (b) strain of a Terfenol-D actuator by varying step input to coil 1 and coil 2.

E. Effect of biasing on steady state static displacement of a Terfenol-D actuator

The output of the Terfenol-D rod is being understood depending on the coils used for biasing. One approach is to maintain constant biasing field to coil 1 and varying step input to coil 2. The second approach keeps the step input to coil 2 constant and biasing field to coil 1 is varied. The maximum displacement of the Terfenol-D rod with mild steel housing is 29.9 µm with constant biasing of coil 1 and varying step input to coil 2. Mean sum of square of error is 0.4 and 0.45 between the experimental displacement during the increase and decrease of biasing step input to coil 1 and coil 2 respectively. This may be also due to the measurement noise for the deviation obtained. It has been concluded that the strain obtained by varying biasing to coil 1 is more than the strain obtained by varying step input to both coils as the net available magnetic field produced by the coaxial coils is more at each excitation. On the other hand displacement achieved is less by varying biasing field to coil 1 when compared to strain achieved with constant biasing to coil 1. It is because, coil 2 is having less number of turns compared to coil 1 and it is also far away from Terfenol-D in the actuator assembly due to which the magneto motive force generated by the coil 2 may not reach effectively to the measuring end of Terfenol-D rod to achieve more strain though the net available magnetic field is same in both cases. It has been summarized that by biasing the magnetic field improves the performance of Terfenol-D actuator as shown in Figure 9.

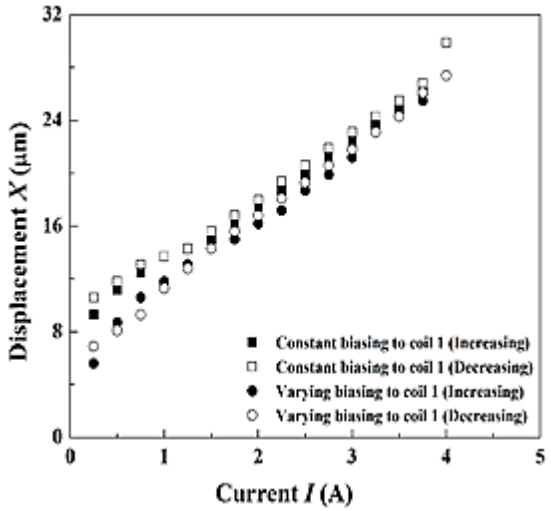

Figure 9. Displacement of a Terfenol-D actuator under biasing conditions.

F. Parameter identification for J-A model

The unknown magnetic and magnetostrictive parameters involved in the magnetization and magnetostrictive model are pinning constant, an-hysteretic parameter, reversibility coefficient, saturation magnetization and saturation magnetostriction. These parameters are associated with the composition and production processes of Terfenol-D rod. In the present work the properties of a Terfenol-D material and the adopted physical parameters are made available from DMRL, Hyderabad. The parameters used in J-A model are listed in Table 3.

S. NO	Parameters	Value
1	Saturation magnetostriction (λ_s)	1350 ppm
2	Saturation magnetization (M_s)	675250 A/m
3	Pinning constant (K)	7000 A/m
4	Anhysteretic parameter (a)	9012
5	Reversibility co-efficient (c)	0.8
6	Applied pre-stress	0, 0.812, 1.624 MPa (0,500,1000 N)
7	Young's modulus (E_s)	30 GPa
8	Dynamic strain co-efficient (d_{33})	15 nm/A [Engdahl, 2000]
9	Saturation pre-stress (σ_s)	200 MPa

I. Magnetostrictive model response curves

The magnetization and magnetostriction responses for a Terfenol-D actuator are discussed using theoretical model. Theoretically the magneto-mechanical characteristics like magnetic field using Equation (21) , magnetization using Equation (28) , strain and displacement using Equation (33) are computed as a function of time. For a step input ranging from 0 A to 4 A under zero prestress conditions results in response curves shown in Figure 10, thus indicates the behavior of different parameters like magnetic field, magnetization, strain and displacement between point of excitation to steady state as a function of time.

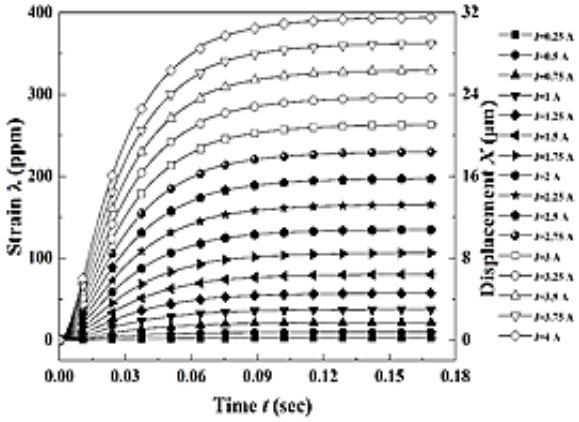

ISSN (Online) 2394-6849

International Journal of Engineering Research in Electronics and Communication Engineering (IJERECE)
Vol 4, Issue 11, November 2017

Figure 10. Response characteristics between Magnetic field and magnetization of an actuator as a function of time.

It is observed that these parameters increase with the increase in applied input DC current from 0 A to 4 A in a step of 0.25 A. Initially the response is transient from the point of excitation to reach till maximum amplitude and thereafter for any time the response is steady. The minimum and maximum displacement obtained are 0.2 and 31.6 µm for an DC input of 0 A and 4 A respectively. It is also observed that the time required for the response to reach from the point of excitation to steady state point is constant as the input increases and equal to 171 ms from Figure 10.

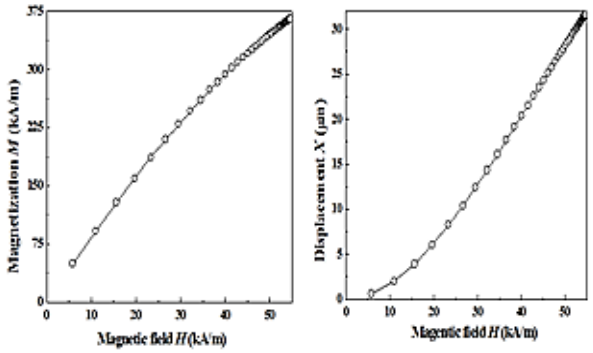

Figure 11. Magnetization curves (a) M vs. H (b) X vs. H of a Terfenol-D actuator.

Figure 11 (a) shows the variation of magnetization against the applied magnetic field. It has been observed that the magnetization keeps on increasing as the magnetic field increases. Magnetization curve shows a non-linear behaviour as the input increased. It has been observed that the displacement increases as the input increased. Its behaviour is non-linear to applied input till 25 kA/m and is proportional to the applied magnetic field beyond 25 kA/m up to 50 kA/m.

J. Comparison of response and magnetization curves with quadratic model

Response and magnetization curves obtained with Equation (28) and Equation (33) are compared with quadratic model given by Equation (29). Figure 12 shows the comparison of displacement against the time. The displacement of the Terfenol-D is obtained for zero preload and step input of 4 A to coil 1 and coil 2. The output displacement obtained with quadratic model which is a function of magnetization alone is more compared to improved magnetostriction model.

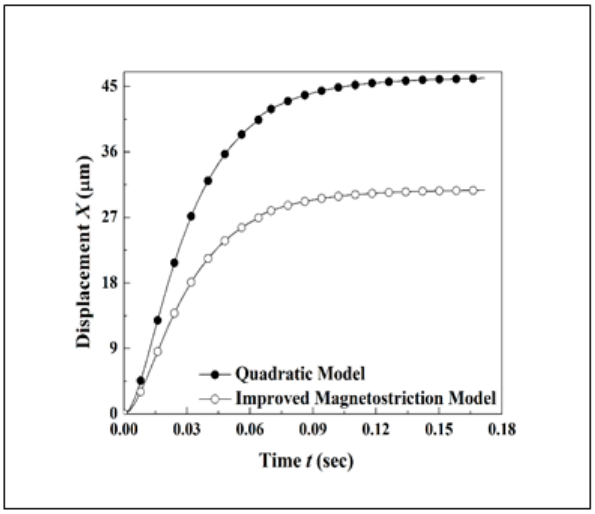

Figure 12. Comparison of theoretical displacement of a Terfenol-D rod as a function of time for a step input of 4 A.

The reason is due to magnetic moments within unfavorable magnetic domains overcome the anisotropy energy and sudden rotation such that one of their crystallographic easy axes is more closely aligned with the external field direction. This sudden rotation is accompanied by a large change in strain.The output from the improved magnetostriction model is an amalgamation of magnetization, applied pre-stress, ΔE effect and the quality factor. The influence of applied pre-stress has been approximated in the form of analytical expression that could closely follow the experimental magnetization. ΔE effect is obvious that will account for the elasticity of the Terfenol-D rod to the applied pre-stress and magnetic field. During the transient response of Terfenol-D rod for the applied step input may undergo longitudinal oscillations and the corresponding frequency could be very close to the resonance. To account for the longitudinal oscillations during transient response, it is proposed to examine the influence of quality factor on the magnetostriction. Figure 12 the outcome of the study is that there is a reduction of 50 % compared to quadratic model. Later it will be observed that the improved magnetostriction model provides the output much close to the experimental output. Figure 13 (a) and (b) shows the comparison of theoretical displacement obtained from Terfenol-D actuator against the applied magnetic field and magnetization. It is observed that the displacement is increasing non-linearly as the applied magnetic field and magnetization increases in case of quadratic and improved magnetostriction models. The maximum displacement of 46 µm and 30 µm has been obtained with quadratic and improved magnetostriction model at an applied input of 4 A respectively.

ISSN (Online) 2394-6849

International Journal of Engineering Research in Electronics and Communication Engineering (IJERECE)
Vol 4, Issue 11, November 2017

H. Theoretical and experimental prediction: Displacement

Figure 14 (a), (b) and (c) shows the comparison of displacement obtained from experiments, quadratic and improved magnetostriction model for a preload of zero, 500 N and 1000 N. The average displacements are 13.5, 17 and 21µm with maximum and minimum values of 0.2, 2.7, 5 µm and 31.5, 36.5 and 41.5 µm have been evaluated using improvised magnetostriction model compared to quadratic model. It may be concluded that the magnetostriction model with all output parameters that affect the output are to be taken in to account due to non-linear hysteretic behaviour of magnetostrictive material. Maximum displacement obtained are 31.5, 36.5 and 41.5 µm with the improved model and 29.9, 34.2 and 38.6 µm from experimental at an applied input of 4 A. Mean sum of squares of errors are 64, 45, 30 between quadratic model and experiment, 5.8, 1.7, 1.4 between improved magnetostriction model and experiment for 0, 500, 1000 N preload conditions.

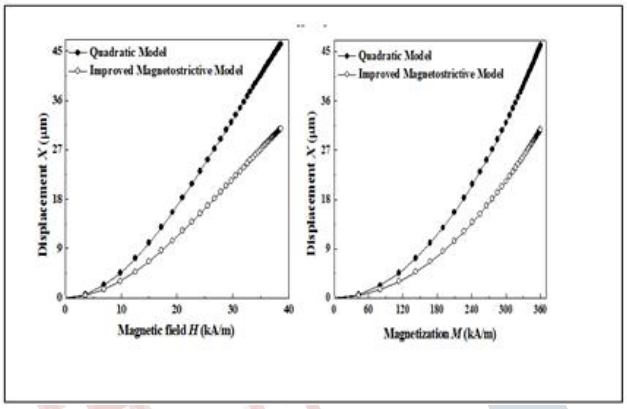

Figure 13. Comparison of theoretical displacement of a Terfenol-D rod as a function of magnetic field (a) and magnetization (b) for a step input of 4 A.

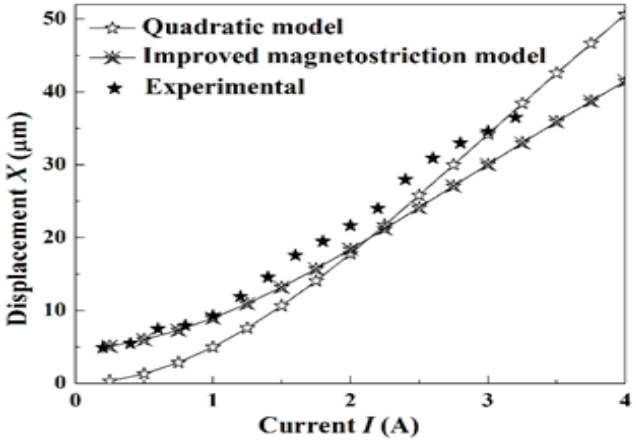

Figure 14. Comparison of theoretical and experimental displacement of a Terfenol-D actuator for different preloads, (a) 0 N (b) 500 N and (c) 1000 N.

Though the magnetostriction model takes as many influencing parameters, the deviation in displacement obtained from experiment has been observed. This may be because of ohmic losses, source instability such as resistance of a coil and air gap present in an actuator among different components due to which there would be flux leakage, are few reasons for the deviation. It is found with that the Jiles-Atherton model along with improved magnetostriction model has provided good estimation on the magnetostriction for the designed actuator.

V. CONCLUSIONS

In the present work, the prototype Terfenol-D actuator has been designed and fabricated. The preliminary experiments under zero pre-stress and pre-stress conditions have been conducted to quantify output displacement of a Terfenol-D actuator. It has been confirmed that the distribution of magnetic flux was stronger by 67 % when the actuator is contained with Terfenol D from the simulation results carried out using Maxwell 2D solver. A biasing magnetic field from coil 1 and intermittent excitation to coil 2 improves the performance of the actuator in comparison to simultaneously varying the input to coaxial coils. Magnetostriction model for the actuator has been improved by adding a quality factor and it is observed that there is a reduction of 50 % in displacement compared to quadratic model. The displacement obtained with the improved model had an average deviation of 6 % with the experimental results. This variation may be due to presence of air gap, flux leakage and fluctuation in the input supply.

REFERENCES

1. Anjanappa, M and Bi, J. 1994. “A theoretical and experimental study of magnetostrictive mini-actuators.” Smart Materials and Structures, 3: 83-91.

2. Brauer, J. R. 2006. “Magnetic actuators and sensors,” A John Wiley & Sons Inc., Publication, Hoboken, New Jersey.

3. BS6722, 1986. “Recommendations for dimensions of ferrous & non-ferrous metallic materials in wire form,” British Standards Institution, ISBN: 0 580 15358 4.

4. Calkins, F. T., Smith, R. C. and Flatau, A. B. 2000. “Energy based hysteresis model for

magnetostrictive transducers," IEEE Transactions on Magnetics, 36(2): 429-439.

5. Calkins, F.T., Flatau, A.B. and Dapino, M.J. 2007. "Overview of magnetostrictive sensor technology." Journal of Intelligent Material Systems and Structures, 18: 1057-1066.

6. Carman, G.P. and Mitrovic, M. 1995. "Non-linear constitutive relations for magnetostrictive materials with applications to 1-D problems." Journal of Intelligent Material Systems and Structures, 6: 673-683.

7. Claeyssen, F., Lhermet, N., Letty, R.L. and Bouchilloux, P. 1997. "Actuators, transducers and motors based on giant magnetostrictive materials." Journal of Alloys and Compounds, 258: 61-73.

8. Dapino, M.J., Smith, R.C., Faidley, L.E., and Flatau. A.B. 2000. "A Coupled structural-magnetic strain and stress model for magnetostrictive transducers." Journal of Intelligent Material Systems and Structures, 11: 135-152.

9. Dapino, M.J., Smith, R.C. and Flatau, A. B. 2000. "Structural magnetic strain model for magnetostrictive transducers." IEEE Transactions on Magnetics, 36(3): 545-556.

10. Dapino, M.J., Smith, R.C., Calkins, F.T. and Flatau. A.B. 2002. "A coupled magnetomechanical model for magnetostrictive transducers and its application to villari-effect sensors." Journal of Intelligent Material Systems and Structures, 13: 737-747.
11. Dehui, L., Quanguo, L. and Yuyun, Z. 2008. "Magnetic circuit optimization design of Giant magnetostricitve actuator." 9th International Conference Computer-Aided Industrial and Conceptual Design, Kunming, 688-692.

12. Dozor, D.M. 1998. "Thermally stable magnetostrictive device." Journal of Intelligent Material Systems and Structures, 9: 732-739.

13. Ekreem, N.B., Olabi, A.G., Prescott, T., Rafferty, A., Hashmi, M.S.J. 2007. "An overview of magnetostriction, its uses and methods to measure these properties." Journal of Materials Processing Technology, 191: 96-101.

14. Engdahl, G. 2000. "Handbook of Giant Magnetostrictive materials," Royal Institute of Technology, Stockholm, Sweden.

15. Engdahl, G. 2002. "Design procedures for optimal use of giant magnetostrictive materials in magnetostrictive actuator applications." 8th International Conference on New Actuators, 10-12 June, Bremen, Germany.

16. Giurgiutiu, V., Rogers, C.A. and Rusovici, R. 1996. "Solid-state actuation of rotor blade servo-flap for active vibration control." Journal of Intelligent Material Systems and Structures, 7: 192-202.

17. Giurgiutiu, V. 2000. "Review of smart materials actuation solutions for aeroelastic and vibration control." Journal of Intelligent Material Systems and Structures, 11: 525-544.

18. Grunwald, A and Olabi, A.G. 2008. "Design of a magnetostrictive (MS) actuator." Sensors and Actuators A, 144: 161-175.

19. Gupta, P.V. 2004. "Introductory course in Electromagnetic Fields," Dhanpat Rai Publications, Taj Press, New Delhi.

20. Jiles, D.C. and Atherton, D.L. 1983. "Ferromagnetic Hysteresis." IEEE Transactions on Magnetics, 19(5): 2183-2185.

21. Jiles, D. C. and Atherton, D. L. 1984. "Theory of ferromagnetic hysteresis," Journal of Applied Physics, 55(6): 2115-2120.
22. Jiles, D. C. and Atherton, D. L. 1986. "Theory of ferromagnetic hysteresis." Journal of Magnetism and Magnetic Materials, 61: 48-60.

23. Karunanidhi. S. and Singaperumal. M. 2010. "Design, analysis and simulation of magnetostrictive actuator and its application to high dynamic servo valve," Sensors and Actuators A: Physical, 57: 185-197.

24. Kellogg, R. and Flatau, A.B. 2004. "Blocked – force characteristics of Terfenol-D transducers." Journal of Intelligent Material Systems and Structures, 15: 117-128.

25. Lhermet, N. and Claeyssen, F., Wendling, P. and Grosso, G. 1993. "Design of actuators based on

biased magnetostrictive rare earth-iron alloys." Journal of Intelligent Material Systems and Structures, 4: 337-342.

26. Liyi. L., Chengming, Z., Baiping, Y. and Xiaopeng, L. 2011. "Research of a giant magnetostrictive valve with internal cooling structure," IEEE Transactions on magnetics, 47 (10): 2897-2900.

27. Olabi, A.G. and Grunwald, A. 2008. "Design and application of magnetostrictive materials," Material and Design, 29: 469-483.

28. Poole, A. D. and Booker, J. D. 2011. "Design methodology and case studies in actuator selection," Mechanism and Machine Theory, 46: 647-661.

29. Rogers, R.C. 1993. "Existence results for large deformations of magnetostrictive materials." Journal of Intelligent Material Systems and Structures, 4: 477-483.

30. Sun, L. and Zheng, X. 2005. "Numerical simulation on coupling behaviour of Terfenol-D rods." International Journal of Solids and Structures, 43: 1613-1623.

31. Wang, L., Ye, H., Liu, Y. T. and Yao, S. M. 2006. "Analysis and optimization for uniformity of magnetic field during the giant magnetostriction," International Symposium on Instrumentation Science and Technology, Journal of Physics, 48: 1336-1340.

32. Wan, Y., Fang, D. and Hwang, K. 2003. "Non-linear constitutive relations for magnetostrictive materials." International Journal of Non-linear Mechanics, 38: 1053-1065.

33. Yong, Y. and Lin, Li. 2009. "Dynamic model considering the ΔE effect for giant magnetostrictive actuators," IEEE International Conference on Control and Automation, Christchurch, New Zealand, 667-672.

34. Yongping, W., Daining, F., Soh, A.K. and Hwang, K.C. 2003. "Experimental and theoretical study of the non-linear response of a giant magnetostrictive rod." Acta Mechanica Sinica, 19(4): 324-329.

35. Young, H. D., Freedman, R. A. and Ford, L. 2007. "University physics with modern physics with mastering physics," 12th Edition, Addison-Wesley Publishers.

36. Zheng, X.J. and Liu, X.E. 2005. "A nonlinear constitutive model for Terfenol-D rods". Journal of applied Physics, 97: 1-8.

37. Zhifeng, T., Fuzai, L. U. and Yang, L. I. U. 2009. "Magnetic field distribution in cross section of Terfenol-D rod and its applications," Journal of Rare Earths, 27: 525-528.

38. Zhou, H. M., Zhou, Y. H. and Zheng, X. J. 2007. "Active vibration control of Terfenol-D rod of giant magnetostrictive actuator with non-linear constitutive relations," Journal of Theoretical and Applied Mechanics, 45(4): 953-967.